Available online at www.sciencedirect.com
ScienceDirect
Remote Sensing of Environment 107 (2007) 385–401
Remote Sensing of Environment
www.elsevier.com/locate/rse

Comparison of MODIS, eddy covariance determined and physiologically modelled gross primary production (GPP) in a Douglas-fir forest stand

Nicholas C. Coops [a,*], T. Andy Black [b], Rachhpal (Paul) S. Jassal [b], J.A. (Tony) Trofymow [c], Kai Morgenstern [b]

[a] Department of Forest Resource Management, 2424 Main Mall, University of British Columbia, Vancouver, Canada V6T 1Z4
[b] Faculty of Land and Food Systems, 2357 Main Mall, University of British Columbia, Vancouver, Canada V6T 1Z4
[c] Canadian Forest Service (Pacific Forestry Centre), Natural Resources Canada, Victoria, British Columbia, Canada V8Z 1M5

Received 14 May 2006; received in revised form 16 September 2006; accepted 17 September 2006

Abstract

Quantification of the magnitude of net terrestrial carbon (C) uptake, and how it varies inter-annually, is an important question with future potential sequestration influenced by both increased atmospheric CO_2 and changing climate. However the assessment of differences in measured and modeled C accumulation is a challenging task due to the significant fine scale variation occurring in terrestrial productivity due to soil, climate and vegetation characteristics as well as difficulties in measuring carbon accumulation over large spatial areas. The Moderate Resolution Imaging Spectroradiometer (MODIS) offers a means of monitoring gross primary production (GPP), both spatially and temporally, routinely from space. However it is critical to compare and contrast the temporal dynamics of the C and water fluxes with those measured from ground-based networks, or estimated using physiological models. In this paper, using a number of approaches, our objective is to determine if any systematic biases exists in either the MODIS, or the modeled estimates of fluxes, relative to the measurements made over an evergreen, needleleaf temperate rainforest on Vancouver Island, Canada. Results indicate that 8-day GPP as predicted with a simple physiological model (3PGS), forced using local meteorology and canopy characteristics, matched measured fluxes very well ($r^2=0.86$, $p<0.001$) with no significant difference between eddy covariance (EC) and modeled GPP ($p<0.001$). In addition, modeled water supply closely matched measured relative available soil water content at the site. Using canopy characteristics from the MODIS fraction of photosynthetically active radiation (fPAR) algorithm, slightly reduced the correspondence of the predictions due to a large number of unsuccessful retrievals (83%) due to sun angle, snow and cloud. Predictions of GPP based on the MODIS GPP algorithm, forced using local meteorology and canopy characteristics, were also highly correlated with EC measurements ($r^2=0.89$, $p<0.001$) however these estimates were biased under predicting GPP. Estimates of GPP based on the most recent MODIS reprocessing (collection 4.5) remained highly correlated ($r^2=0.88$, $p<0.001$) yet were also the most biased with the estimates being 30% less than the EC-measured GPP. Most of the variance in GPP at the site was explained by the absorbed photosynthetically active radiation. We also compared the nighttime respiration as measured over 2 years at the site with the minimum 8-day MODIS land surface temperature and found a significant relationship ($r^2=0.57$), similar to other studies.
© 2006 Elsevier Inc. All rights reserved.

Keywords: Gross primary productivity; MODIS; Physiological modelling; 3PGS; fPAR

1. Introduction

The terrestrial biosphere can sequester significant amounts of atmospheric CO_2 (Wofsy et al., 1993) with future potential sequestration influenced by both increased atmospheric CO_2 and changing climate (Nemani et al., 2003, 2002). As a result, quantification of the magnitude of the net terrestrial carbon (C) uptake, and how it varies inter-annually, is an important question facing the ecological and global climate change communities (Barford et al., 2001; IPCC, 2001). As the magnitude of this uptake remains uncertain, understanding the C cycle at local, regional and global scales requires Earth surface processes to be monitored at high spatial and temporal resolutions (Zhao et al., 2005). Globally, the Moderate

* Corresponding author. Tel. +1 604 822 6452; fax: +1 604 822 9106.
E-mail address: nicholas.coops@ubc.ca (N.C. Coops).

0034-4257/$ - see front matter © 2006 Elsevier Inc. All rights reserved.
doi:10.1016/j.rse.2006.09.010

Resolution Imaging Spectroradiometer (MODIS), on board the TERRA and AQUA platforms, is a critical tool providing a monitoring capacity of the C cycle as part of the NASA Earth Observing System (Zhao et al., 2005). The MODIS sensors, launched in 1999 and 2001, provide a near daily coverage of the globe at 1-km resolution in 36 spectral bands (Heinsch et al., 2006) and include state of the art geo-location, atmospheric correction and cloud screening provided by MODIS science team. Using the MODIS instrument, estimates of foliage characteristics can be determined using visible and near-infrared spectral wavelengths and this, combined with global meteorology and a set of biome-specific parameters, which simulate vegetation growth under a range of conditions, allow the estimation of gross primary productivity (GPP), the photosynthetic accumulation of C by plants.

Ultimately, the value and utility of such datasets for environmental and C modeling is determined by our ability to quantify and explain uncertainties in the MODIS predictions. However the assessment of differences in measured and modeled C accumulation is a challenging task due to the large fine scale variation occurring in terrestrial productivity due to soil, climate and vegetation characteristics (Gebremichael & Barross, 2006) as well as difficulties in measuring C accumulation over large spatial areas.

To meet this end, a global ground based monitoring network of micrometeorological tower sites is in place that use eddy covariance (EC) fluxes to estimate gross primary productivity (GPP) as the sum of net ecosystem production (NEP) and ecosystem respiration during daylight periods (Goulden et al., 1996; Turner et al., 2003). Towers operate in many countries, across all continents, through a network known as FLUXNET, (Baldocchi et al., 2001) and at present, over 200 tower sites are operating on a long-term and continuous basis, with data colleted on fluxes as well as vegetation, soil, hydrologic, and meteorological characteristics. In addition to MODIS satellite predictions, and ground based measurements, a third approach to the determination of site-level GPP, is to estimate C exchange through the use of ecosystem process-based models using a range of site-level measured meteorological, biophysical, and soil inputs (Friend, 1995; Garcia-Quijano & Barros, 2005; Running & Gower, 1991). Such models incorporate an understanding of physiological processes and predict the growth and respiration of plant tissue. With adequate data, model estimations can be scaled both spatially and temporally, allowing for comparisons of the spatial pattern, and seasonal to inter-annual variability, of vegetation activity to be assessed (Heinsch et al., 2006; Schimel, 1995).

Validation and verification of the MODIS GPP product is underway. Turner et al. (2003) compared 2001 MODIS GPP with GPP estimates based on model-scaled ground observations at temperate hardwood and boreal conifer forested sites. The ground-based GPP scaling approach relied on a C cycle process model, BIOME-BGC, run in a spatially distributed mode (Turner et al., 2003). At the hardwood forest site, the MODIS GPP phenology started earlier than the scaled modeled GPP, and the summertime MODIS GPP was generally lower than the scaled modeled GPP values. The timing of the MODIS fall-off in production at the end of the growing season was similar to the validation data. At the boreal forest site, the MODIS and scaled model GPP phenologies generally agreed as both responded to the strong signal associated with minimum temperature. The boreal midsummer MODIS GPP was generally higher than the scaled model GPP values. The differences between the MODIS and the scaled model GPPs were driven by seasonal changes in the fraction of photosynthetically active radiation (fPAR) and the magnitude of the light use efficiency (ε) as well as by differences in other inputs to the MODIS GPP algorithm such as radiation, minimum temperature, and vapor pressure deficit (VPD). As a follow on to this work Turner et al. (2005) evaluated MODIS production estimates across six sites with varying climate, land use, and vegetation physiognomy, and compared them to estimates derived from a combination of ground measurements, Landsat imagery and process modelling (BIOME-BGC). There was not a consistent over- or under-prediction of production across sites relative to the validation estimates. Closest agreement occurred at the temperate deciduous forest, arctic tundra, and boreal forest sites with overestimation at the desert grassland and at the dry coniferous forest sites. Gebremichael and Barross (2006) evaluated the MODIS GPP estimates in two tropical ecosystems: a mixed forest site in the humid tropics and an open shrubland site in a semi-arid region using a process-based biochemical-hydrology model (LEHM, Land EcoHydrology Model) driven by flux tower meteorological observations. Results indicated there was a positive bias in predictions for the mixed forest biome and a negative bias for the open scrublands due in part to the global meteorology used by the MODIS algorithm. Heinsch et al. (2006) has undertaken a comprehensive evaluation of the MODIS GPP product using estimates derived from measured net ecosystem exchange (NEE) at a number of flux towers across North America. In this comparison, 4 years of MODIS GPP data were compared at 15 sites covering a range of biome types. The results indicted that, relative to the tower-based estimates, MODIS overestimated GPP by an average 20–30% at most of the sites with intra-annual variability varying by time-scale and biome. The results also indicated however MODIS substantially underestimated GPP between 19% and 40% at the most productive site (the Duke Forest site, North Carolina consisting of evergreen needleleaf forest). These results indicate that the combined underestimation of VPD from inadequate global meteorological data and the lack of accounting for soil moisture within the MODIS GPP algorithm leads to errors in estimating GPP and to difficulties in capturing seasonal dynamics, particularly for water-limited sites across the U.S.A. (Baldocchi et al., 2001; Heinsch et al., 2006; Turner et al., 2003). In the case of the higher productivity sites the maximum radiation conversion use efficiency, ε, was likely underestimated and conversely reductions imposed by the minimum temperature and VPD overestimated.

In this paper, we utilize a combination of EC-measured, physiological model, and satellite model (MODIS) derived estimates of GPP and compare the temporal dynamics of the C fluxes at 8-day, seasonal and annual intervals. By using a combination of ground-based and satellite observations, our

objective is to determine if any systematic biases exists in either the MODIS, or the modeled estimates of fluxes, relative to the EC observations taken at the flux tower. Our long-term objective is to develop an improved understanding for quantifying the spatial patterns and temporal changes in GPP of terrestrial ecosystems at large spatial scales.

2. Study area and data

2.1. Study area

The study was conducted in Douglas-fir (*Pseudotsuga menziesii* (Mirbel) Franco) and western hemlock (*Tsuga heterophylla* (Raf.) Sarg.) forests within the Oyster River area located near Campbell River on leeward eastern side of Vancouver Island, British Columbia. This location is the site of the Campbell River EC flux tower, established in 1996 and managed by the University of British Columbia (UBC) and part of the Fluxnet Canada Research Network (FCRN, site name DF1949) (Humphreys et al., in press). The site is located within the dry maritime Coastal Western Hemlock biogeoclimatic subzone (CWHxm), which has annual precipitation averaging 1500 mm and annual temperature of 9.1 °C (Pojar et al., 1991). This subzone has a maritime climate with typically cool summers and mild winters, though can experience significant dry conditions during the summer. Douglas-fir is the dominant tree species around the EC tower site, though wetter site series also containing western hemlock and western red-cedar (*Thuja plicata*) occur within 1 km (Green & Klinka, 1994). Stand basal area ranges from 50–60 m^2 ha^{-1}, live stem densities range from 675–1900 trees ha^{-1}, and mean dominant tree heights range from 24 m–33 m. Forests within the tower footprint are second-growth, arising after harvest (1937 and 1943) and slash-burning (1939 and 1943) of the original old-growth forest. Much of the site did not regenerate naturally (Goodwin, 1937) with the forest stand near the tower established by planting in 1949, and stands in the periphery establishing naturally or by planting between 1942 and 1961. The entire site was fertilized once in 1994 with 200 kg N. The site is steeply to strongly sloping (5–25%), ranges in elevation from 275 m–385 m, and with gravely sandy loam textured duric humo-ferric soils of morainal origin (Jungen, 1985) of over 1 m in depth.

2.2. CO_2 fluxes

Since September 1997, half-hourly fluxes of CO_2, water vapor and sensible heat above the canopy have been measured continuously using the EC technique from a 45 m tall, 51 cm triangular open-lattice type tower. In addition, a large number of meteorological observations, including downwelling and upwelling shortwave and longwave radiation (from which net radiation was calculated), downwelling and upwelling photosynthetically active radiation, air temperature, relative humidity, and rainfall, have been recorded at each 30 min time interval. A detailed description of the study site, and the data collection, processing and archiving at the site is available in Morgenstern et al. (2004). Half-hourly values of GPP were calculated using:

$$\mathrm{GPP} = \mathrm{NEP} + R_\mathrm{d}$$

where NEP is the daytime net ecosystem production and R_d is the daytime ecosystem respiration. The former was obtained from NEE (i.e., NEP = −NEE) which was calculated as the sum of the CO_2 flux measured by EC at the top of the tower and the rate of change in CO_2 storage in the air column beneath the EC sensors. Using the measured daytime soil temperature at the 5-cm depth, R_d was calculated with the annual relationship between nighttime NEE (i.e., ecosystem respiration) measured when atmospheric turbulent mixing was adequate (friction velocity > 0.3 m s^{-1}) and nighttime soil temperature at the 5-cm depth (Morgenstern et al., 2004). We used data for the 5-year period, 2000–2004 available from the FLUXNET Canada website (http://www.fluxnet-canada.ca/). Flux data were gap filled using the procedure described in Barr et al. (2004) except that rather than using a logistic respiration versus temperature relation an exponential relation was used (Morgenstern et al., 2004). Gap-filled half hourly values of GPP were summed to give either daily or average 8-day total fluxes in kg C m^{-2} day^{-1} for comparison with MODIS predicted GPP values.

2.3. Measurement of soil water content and estimation of available water content

Half-hourly measurements of soil water content (θ) were made using CSI water content reflectometers (Model CS-615, Campbell Scientific Inc., Logan, UT, USA) at two locations close to the tower by installing four of these sensors at each location at four depths between 2 and 100 cm. In addition, 11 stations of time domain reflectometry (TDR) probes (Hook & Livingston, 1996) integrating the top 30 cm and the top 70 cm of the soil profile was manually measured monthly with a cable tester (Model 1502B, Tektronix, Beaverton, OR) and used to account for the spatial variability in soil water content.

Several approaches have been used to analyze the effects of water stress on vegetation. Baldocchi (1997) introduced an empirical drought index derived from the ratio of cumulative potential evaporation to cumulative precipitation (P). Griffis et al. (2003) used cumulative P/E, where E is the evapotranspiration, as an upper limit of the amount of water available for tree growth. Reichstein et al. (2002) suggested using the ratio of volumetric soil water content, θ, and soil water content at field capacity, θ_fc, to determine drought effects. In the present study, relative available soil water content is used to characterize the impact of water stress. Generally, plant water uptake remains high until about one-half of the available water has been extracted (Campbell & Norman, 1998; Foti et al., 2003). Black (1979) measured evapotranspiration in a Douglas-fir stand and found that ratio of the evapotranspiration rate to the equilibrium evaporation rate began to decrease when extractable water in the root zone was reduced to 40%, and the ratio tended to be zero when soil water potential exceeded 1.5 MPa.

Plant available water (θ) in the soil was therefore calculated as $\theta_\mathrm{fc} - \theta_\mathrm{wp}$ where θ_fc and θ_wp are the volumetric soil water content at "field capacity" and "permanent wilting point" respectively. As an index of soil water availability for plant growth, we calculated "relative available water content", θ_ra as $\theta_\mathrm{ra} = (\theta - \theta_\mathrm{wp})/(\theta_\mathrm{fc} - \theta_\mathrm{wp})$.

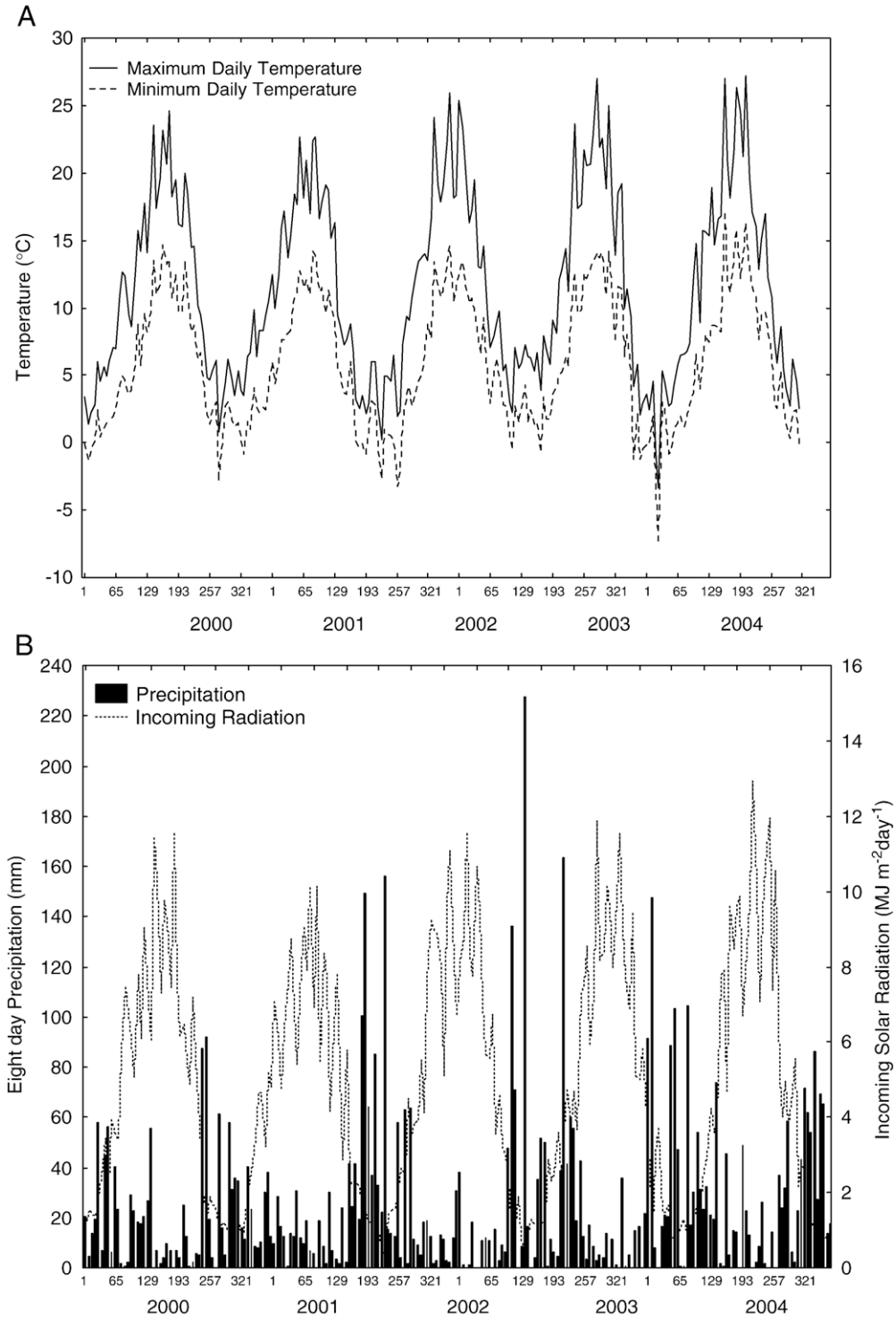

Fig. 1. Meteorological data collected at the flux tower site from 2000–2004. 1(A) 8-day minimum and maximum air temperature (°C) and (B) 8-day accumulated precipitation (mm) and average daily photosynthetically active radiation (MJ m^{-2} day^{-1}).

Soil water characteristics (soil water content–soil matric potential relationships) were determined on intact soil cores from 0–30 and 30–60 cm layers in the laboratory using pressure plate apparatus. From these measurements, estimates θ_{fc} and θ_{wp} for the 0–60 cm soil layer were obtained to be 0.25 and 0.10 m^3 m^{-3} respectively, which we used to calculate θ_{ra} to specify the fraction of available water in the 0–60 cm soil layer.

2.4. Meteorological data

In addition to fluxes, meteorological data including half hourly estimates of air temperature (°C), precipitation (cm), total incoming shortwave radiation (W m^{-2}) and relative humidity (%) were used in the analysis (Fig. 1). The amount and distribution of rainfall differs from year to year and needs

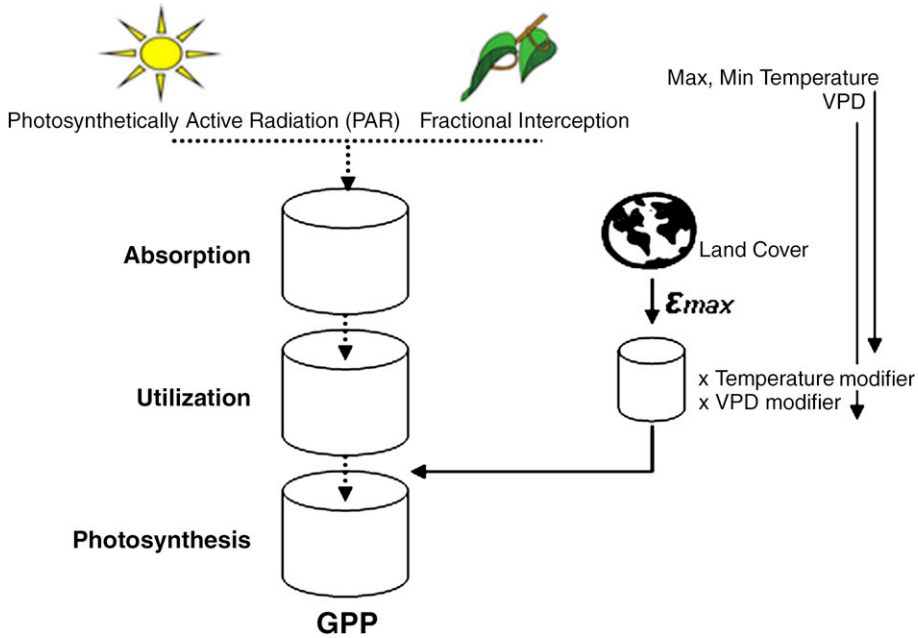

Fig. 2. Flow diagram of the major processing steps of the MODIS GPP algorithm.

to be interpreted in the context of the long-term climatic variability for the site. Mean annual rainfall for the period 1940–2002 is 1450 mm. Over the 5 years of interest (2000–2004), only 2004 experienced above average rainfall with 2001 and 2002 being lower than average (approximately 1200 mm). Total incoming radiation as expected remained relatively constant over the 5 years peaking at 14 MJ m^{-2} day^{-1}. Mean 8-day maximum and minimum temperatures remained more constant over the 5 years period than rainfall. Generally over the 5 years, temperatures have slightly increased from the coolest in 2000 to the warmest year in 2004, from a monthly maximum average of 10.7 °C in 2000 to 11.4 °C in 2004.

3. Overview of GPP algorithms

3.1. Estimation of GPP using the MODIS algorithm

The MODIS GPP algorithm is described in detail by Running et al. (2004), requiring only brief coverage here. The algorithm relies on the light-use efficiency approach relating GPP to the amount of absorbed photosynthetically active

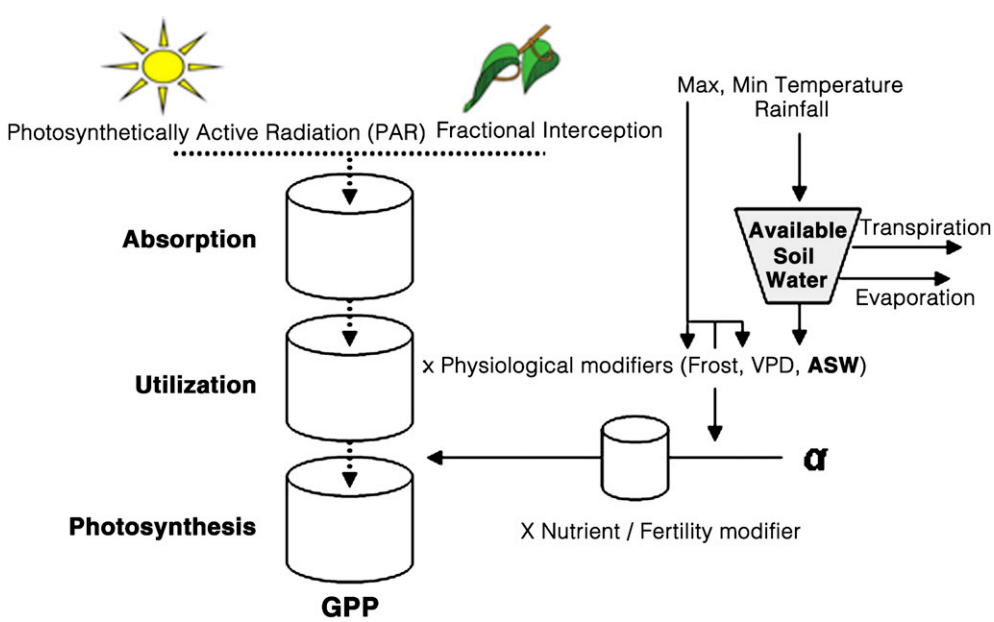

Fig. 3. Flow diagram of the major processing steps of the 3PGS GPP algorithm.

radiation (APAR) (Monteith, 1966, 1972) through the use of a maximum radiation use conversion efficiency term (ε) (kg C MJ^{-1}) such that:

$$GPP = \varepsilon \times f\,PAR \times PAR$$

where fPAR is the fraction of incident PAR absorbed by the canopy (between 0 and 1), and PAR is the flux density of photosynthetically active radiation (MJ m^{-2} day^{-1}).

The maximum value of ε is dependent on vegetation type (as defined by the MODIS land cover classification) and is reduced by two multipliers based on climate. One which reduces the conversion efficiency when cold temperatures limit plant function, and the second which reduces the maximum conversion efficiency when the VPD is high enough to inhibit photosynthesis. Both multipliers range from 0 (total inhibition) to 1 (no inhibition). Whilst the effect of soil water availability is not included in the MODIS GPP algorithm, sensitivity to VPD is increased in the model as a surrogate for drought effects (Heinsch et al., 2006), (Fig. 2).

The MODIS GPP algorithm requires input data from three sources. Biome specific parameters such as ε, are assigned based on an 8 class 1 km pixel MODIS land cover classification and the associated Biome Parameter Look Up Table (BPLUT) (Hansen et al., 2000; Running et al., 2004). Incoming radiation is obtained along with air temperature and relative humidity from global scale meteorology (1.00°×1.25°) via NASA's Data Assimilation Office (DAO) GEOS-4 global climate model (DAO, 2002). Whilst these data have a much coarser spatial resolution than the 1 km MODIS products, there is an implicit assumption that the coarse resolution meteorological data still provides accurate depictions of the surface boundary layer conditions and that these conditions are homogeneous within the spatial extent of each cell (Gebremichael & Barross, 2006). The third dataset is the prediction of daily fPAR, which comes directly from a structural land cover map and atmospherically corrected surface reflectances at a 1 km resolution from MODIS spectral bands as well as information on viewing and illumination angles (Myneni et al., 2002). Daily MODIS GPP estimates are derived by summing the daily intermediate GPP values over an 8-day period for the first 45 values/year and over 5 days (or six in a leap year) during the final period and then averaging to produce a daily predicted GPP product each 8 days.

Three potential sources of error related to inputs for the MOD17 GPP algorithm are: (1) meteorology, (2) radiometry, and (3) biophysical inputs to the model (Heinsch et al., 2006). Meteorological errors arise from the coarse scale meteorology from the DAO. Errors in radiometry can cause miscalculations in the fPAR algorithm and finally misclassification in the land cover classification. Errors in either of these classification schemes will lead to incorrect estimates of GPP (Heinsch et al., 2006). More details on the fPAR errors are discussed in the fPAR section.

3.2. Estimation of GPP using the 3PGS model

The 3PGS (*P*hysiological *P*rinciples *P*redicting *G*rowth from *S*atellites) model (Coops et al., 1998) is a simplified version of the original implementation of the 3-PG model (Landsberg & Waring, 1997) and is driven primarily by vegetation light absorption, which determines the potential physiological rates. 3PGS uses many of the principles that underlie earlier models such as FOREST-BGC (Running & Coughlan, 1988), and BIOMASS (McMurtrie et al., 1990). Like these models, and the MODIS algorithm, 3PGS first estimates absorbed photosynthetically active radiation (APAR) as the product of incident PAR (photosynthetically active radiation) and the fraction of PAR absorbed by the forest canopies (fPAR), which is normally estimated from a satellite-derived index. 3PGS then calculates the utilized portion of APAR by reducing APAR by an amount determined by the most constraining of a series of environmental modifiers that affect gas exchange through stomata, viz. (a) high day-time atmospheric VPD (b) soil water availability, and (c) the frequency of sub-freezing temperatures (<−2 °C). In addition, photosynthesis is further constrained by suboptimal temperatures that reduce the maximum quantum efficiency (α), determined by the availability of nutrients, specifically nitrogen. In the initial implementation of the model, GPP is calculated at monthly time steps as the product of APAR and α, the 'effective' (suboptimal temperature adjusted) quantum efficiency (Landsberg & Waring, 1997) (Fig. 3).

Unlike the MODIS GPP algorithm, 3PGS utilises a soil water balance model calculated water stress as the difference between total monthly rainfall, plus available soil water stored from the previous month, and transpiration, calculated using the Penman–Monteith equation with canopy conductance modified by the leaf area index (LAI) of the forest and constrained by monthly estimates of *D* (Coops & Waring, 2001a,b).

The 3PGS model was originally developed to run at a monthly time-step, chosen as a compromise between capturing canopy photosynthetic characteristics, input data requirements and being sufficiently quick to allow simulations for 100–200 years. In order for the model predictions to be compared with those of the MODIS GPP algorithm an 8-day time step

Table 1
3PGS Douglas-fir calibration parameters

Variable	Functions and parameter values	Reference
Light conversion of photosynthesis	Maximum α_c set to 0.057 mol C mol^{-1} photons	Lewis et al. (1999)
Temperature	T_{opt} was set at 20 °C, T_{min} at −5 °C and T_{max} at 40 °C	Lewis et al. (1999)
Soil fertility rank (FR) (0 to 1)	1.0	This study
Available soil water storage (θ_{max})	250 mm	This study
Canopy boundary layer conductance	0.09 m s^{-1}	White et al. (2000)
Maximum leaf stomatal conductance	0.08 m s^{-1}	Waring and McDowell (2002)
Maximum canopy stomatal conductance (g_{cmax})	0.018 m s^{-1}	Waring and McDowell (2002)
Stomatal response (g_c) to vapor pressure deficit (kPa)	$g_c = g_{cmax}\exp(-0.5VPD)$	Landsberg and Waring (1997)

implementation of the 3PGS model was developed for this paper, utilizing the same processing steps, however, using 8-day meteorological observations. 3PGS therefore models the soil water balance as the difference between total 8-day transpiration and accumulated 8-day precipitation. The model is initialized with soil water content = maximum available water (θ mm) in the soil profile (Landsberg & Gower, 1997), in this case 0–60 cm. The moisture ratio (r_θ) for the stand is calculated as r_θ = (total available soil water content + water balance[difference between total transpiration and precipitation])/(maximum available water). The water balance at each 8-day time step will be negative if transpiration exceeds precipitation, and vice versa (Coops & Waring, 2001b; Landsberg & Waring, 1997). Waring and McDowell (2002) parameterised the 3PG model for Douglas-fir including optimum, minimum and maximum temperature ranges, leaf and canopy response to D. Values for α were obtained from Lewis et al. (1999), and boundary layer conductance from White et al. (2000). Parameterisations used in this application of the 3PGS model implementation are shown in Table 1.

3.3. Measurement and prediction of fPAR

Both the MODIS GPP algorithm and the 3PGS model require regular input of information on the fPAR absorbed by vegetation. fPAR is a function of both canopy properties and solar zenith angle, and as a result can vary diurnally as well as seasonally (Chen, 1996). As part of ongoing research at the Campbell River tower site, LAI was measured along two transects from the tower using the TRAC (Leblanc & Chen, 2001) instruments. As a result, effective LAI and element clumping index were measured and the effective LAI of the Douglas-fir stand in the flux footprint area around the tower was found to be 5.6 (Chen et al., in press). Based on this corrected LAI, the fPAR of the stand can be computed, for any day of the year using the following equation (Chen, 1996):

$$f\,\mathrm{PAR} = 1-\rho_1-(1-\rho_2)e^{(-0.45L_{\mathrm{eg}}/\cos\theta)}$$

where ρ_1 and ρ_2 are species specific constants, L_{eg} is the effective green LAI, and θ is the solar zenith angle. ρ_1 and ρ_2 were found to be 0.05 and 0.06 respectively for conifer stands (Chen, 1996). For simplicity, a constant value of 0.45 is used for the extinction coefficient for the global PAR and L_{eg} is the measured LAI (multiplied by a factor of 1.16 to account for the effect of multiple scattering which, in complex conifer canopies, can deviate from the spherical distribution to a considerable extent (Chen, 1996)).

Currently the MODIS GPP algorithm utilizes the MOD15A dataset which provides 8-day fPAR observations. The MODIS fPAR algorithm retrieves fPAR from daily surface reflectance data in the red (648 nm) and near-infrared (858 nm) regions of the spectrum at a 1 km resolution. The main algorithm performs retrievals based on a radiative transfer algorithm, information on sun angle and view directions and the Bidirectional Reflectance Factor (BRF) for the relevant biome land cover class. The computed estimates of fPAR are then compared to a suite of values which represent an expected range of typical conditions for a given biome type. The algorithm, however, may fail if input reflectance data uncertainties are greater than preset threshold values in the algorithm or due to deficiencies in model formulation which result in incorrect simulated BRFs (Tian et al., 2002). The major reason for poor retrievals of fPAR information is cloud and snow cover since the main fPAR algorithm cannot

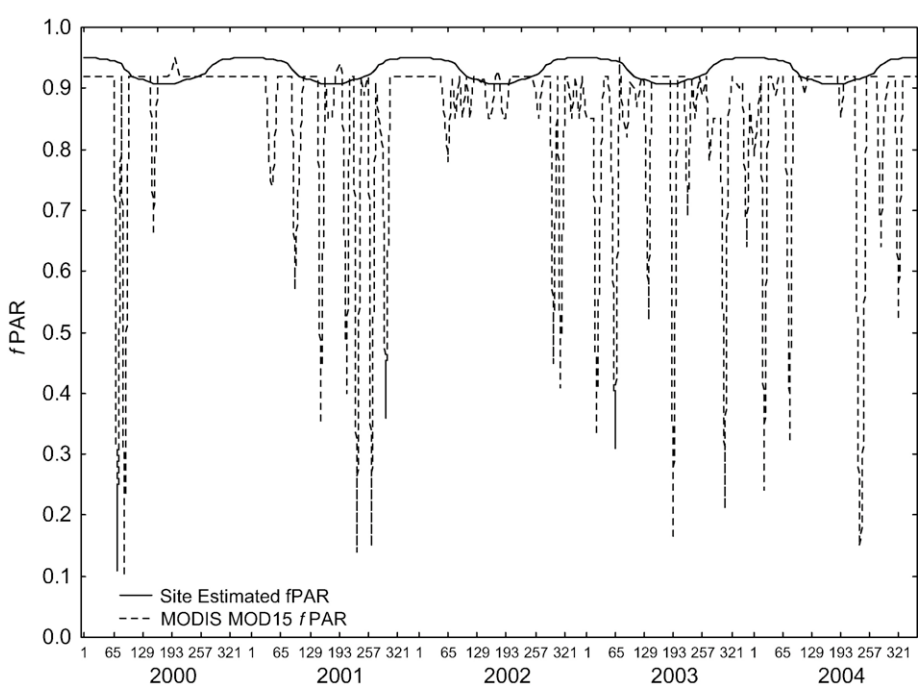

Fig. 4. 8-day fPAR as derived from the MOD15A product at the Campbell River site, as well as predictions of fPAR variation based on the approach of Chen (1996) using variable solar angle calculations and a constant LAI based on the August 2005 field observations.

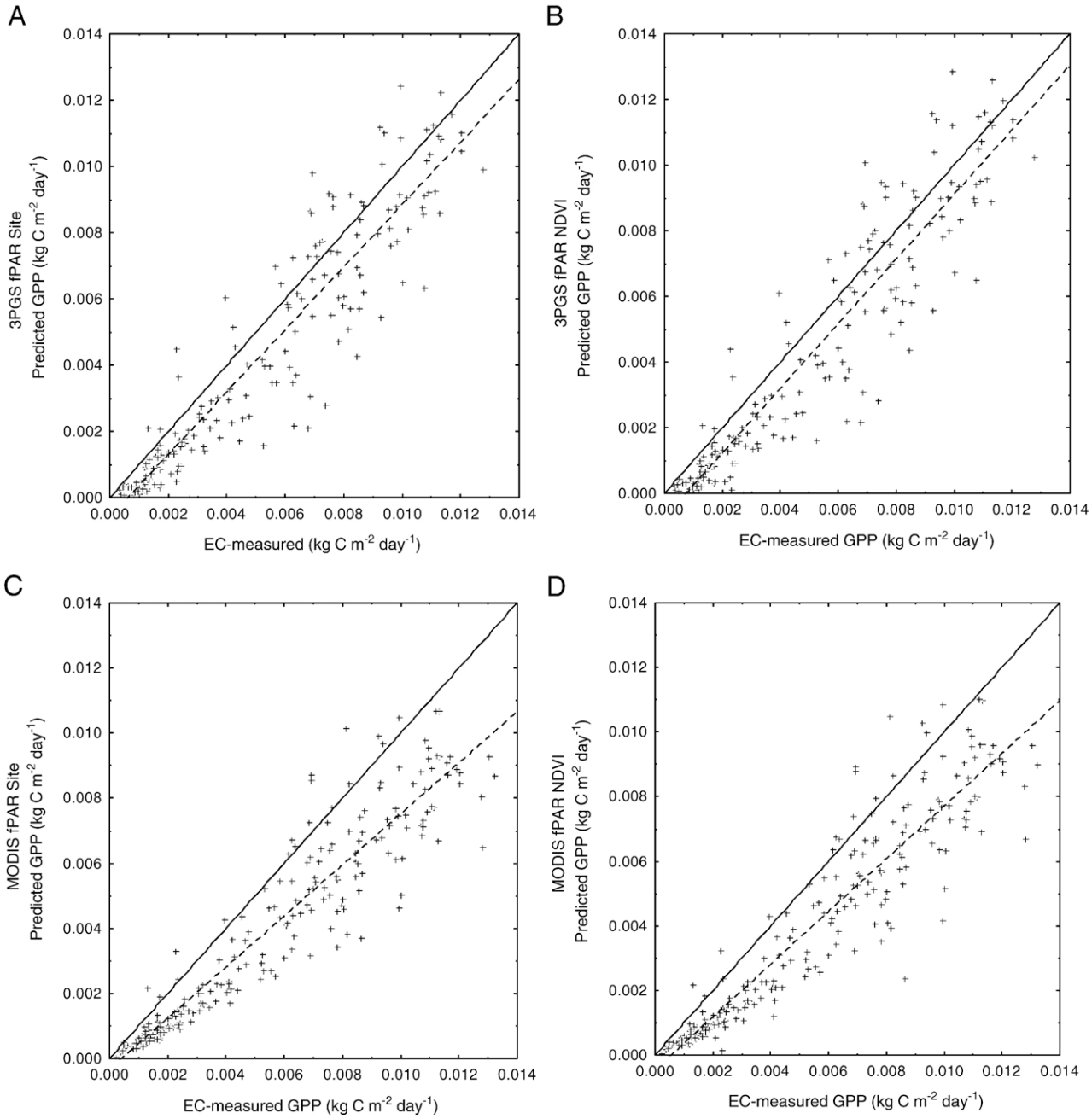

Fig. 5. (A)–(D) Comparison of the EC-measured 8-day GPP with (A) 3PGS predictions of GPP using local meteorology and site estimates fPAR (3PGS fPAR Site), (B) 3PGS predictions of GPP using local meteorology and NDVI backup fPAR (3PGS fPAR NDVI), (C) MODIS algorithm predictions of GPP, using local meteorology and site estimated fPAR (MODIS fPAR Site) and (D) MODIS predictions of GPP, using local meteorology and NDVI backup fPAR (MODIS fPAR NDVI). In all cases the dashed line is the linear best fit and the solid line is the 1:1 reference.

handle observations when the pixel's reflectance data are corrupted due to the presence of clouds or other atmospheric effects (Myneni et al., 2002). In the case of snow cover, the main algorithm retrieval rate is 2.5–5% due to the fact that snow significantly increases both red and near-infrared reflectance such that NDVI is close to 0. In all such cases, the retrievals are generated by a back-up algorithm based on biome-specific empirical relationships between the NDVI and fPAR described in detail in Knyazikhin et al. (1999). To minimize the influence of cloud cover and other unfavorable conditions, the maximum daily fPAR across each 8-day period is selected as the representative daily fPAR for the period, assuming that the fPAR does not change. Recent analysis has shown that globally the success of the main algorithm to retrieve fPAR is 70% (Yang et al., 2006).

MODIS products have undergone a number of revisions (known as collections) since the first satellite launch. The most recent re-processing for GPP is collection 4.5 which includes a more rigid assessment of MODIS fPAR predictions prior to inclusion in the GPP algorithm. In the case of the collection 4.5 only reliable fPAR values (i.e., obtained using the main fPAR

Table 2
Average daily, and standard deviation, eddy covariance (EC) measured, MODIS and 3PGS modelled GPP (kg C m^{-2} day^{-1}) derived using a range of fPAR and meteorological inputs (MODIS fPAR and GPP data for 1 km cell centred over flux tower location)

GPP methods	Met. data source	Mean (kg C m^{-2} day^{-1})	SD (kg C m^{-2} day^{-1})	r^2	SE (kg C m^{-2} day^{-1})
EC-measured	Local	0.005269	0.003501		
3PGS fPAR Site	Local	0.004428	0.003585	0.86	0.0009
3PGS fPAR MODIS	Local	0.004199	0.003647	0.80	0.0015
3PGS fPAR NDVI (backup)	Local	0.004490	0.003737	0.86	0.0009
MODIS fPAR Site	Local	0.003879	0.002952	0.89	0.0010
MODIS fPAR MODIS	Local	0.003634	0.003013	0.80	0.0014
MODIS fPAR NDVI (backup)	Local	0.003927	0.003086	0.90	0.0011
MOD17 C 4.5	DAO	0.002968	0.002600	0.88	0.0010

Also shown is the coefficient of determination (adjusted r^2) and standard error of relationship between 3PGS and MODIS estimated GPP with EC-measured GPP.

algorithm) are used in the estimation of GPP. When there are no reliable LAI/fPAR values over the span of 8 days, the corresponding value is determined through linear interpolation between the previous period's value and that of the next good period. Detailed information on these algorithms is given in Zhao et al. (2005).

3.4. MODIS land surface temperature

Given the recent success of Rahman et al. (2005) in utilizing land surface temperature in the estimation of nighttime respiration, we took advantage of this comprehensive CO_2 and water flux dataset to examine the extent of a general relationship between ecosystem nighttime respiration and MODIS surface temperature that could be used for direct estimation of per-pixel respiration.

3.5. Extraction of MODIS data

This research is based on Collection 4.5 MODIS GPP data, available from the University of Montana and Oak Ridge National Laboratory (ORNL) Distributed Active Archive Center (DAAC). We obtained 7 km × 7 km cut-outs centered over the Campbell River flux tower site location representing:

- 8-day, 1 km, LAI and fPAR (MOD15, C4) [2000–2004],
- MODIS land surface temperature (MOD11) [2000–2004],
- MODIS 16 day 1 km NDVI [2000–2004],
- GPP (MOD17, C4.5) [2000–2003].

Eight day mean, seasonal, and total annual values of GPP were calculated for the central pixel centred over the flux tower location.

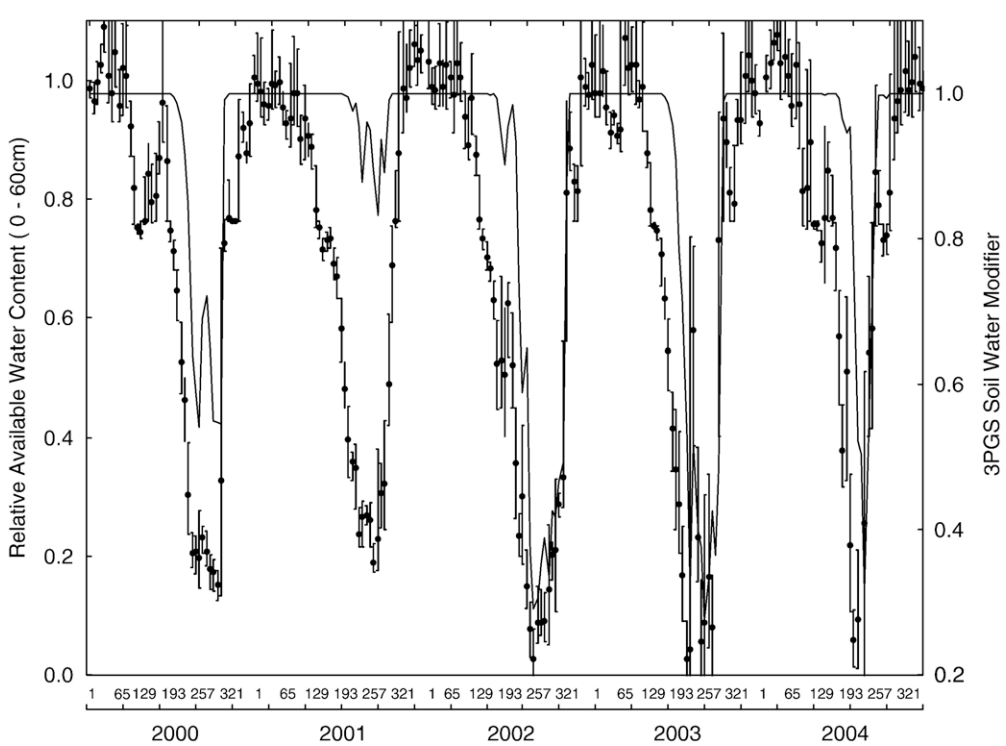

Fig. 6. 3PGS model predictions (using local meteorology and site based fPAR) of the soil water modifier (right axes, solid line) and the 8-day mean (●), minimum and maximum relative soil water content in the 0–60 cm layer measured at the site (left axis).

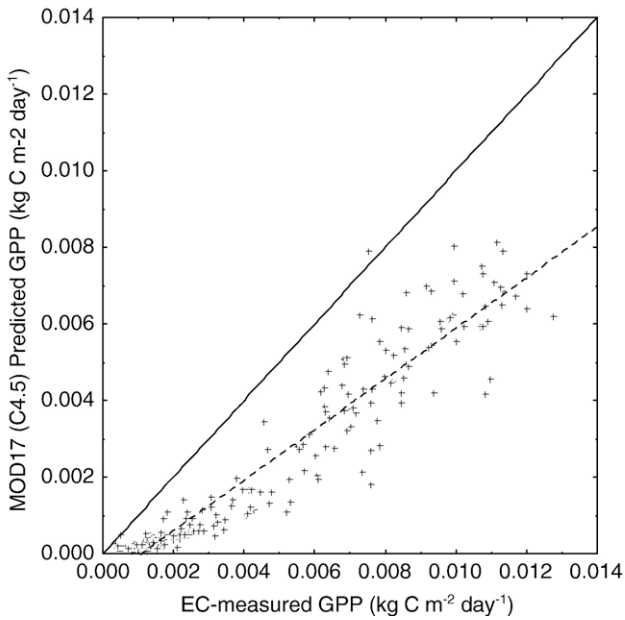

Fig. 7. Comparison of the EC-measured 8-day GPP with MOD17 predictions of GPP (kg C m^{-2} day^{-1}). The dashed line is the linear best fit and the solid line is the 1:1 reference.

In addition, data on the quality assurance flags for the single, and the 7×7 km subset were obtained and analysed. MODIS data collection began on day 56 of 2000; therefore to have four complete years of GPP data, average reliable LAI and fPAR were calculated from the 2001–2003 data and used to simulate GPP estimates for January–February 2000 (Zhao et al., 2006). MODIS fPAR 8-day composites were available from 2000–2004 allowing 5 years of comparisons with 3PGS modeled and with EC-measured GPP. In situations where the MODIS fPAR 8-day composites were tagged as un-reliable, we extracted the nearest cloud-free NDVI cell within 7×7 km subset, and computed the fPAR based on the relationships provided in Knyazikhin et al. (1999). Land surface temperature 8-day averages at 1 km resolution were also extracted for each 7×7 km area over the tower location and valid values averaged to produce a spatially averaged mean 8-day land surface temperature. This was then compared with the 8-day nighttime respiration as measured at the tower location following the procedure of Heinsch et al. (2006).

4. Results

Analysis of fPAR returns from the MOD15, C4 product indicated that only 17% of fPAR retrievals were derived from the main algorithm (using directionally corrected reflectances). As a result the majority of the retrievals for the Campbell River site in the MODIS 4.5 GPP product are either interpolated over significant 8-day time steps or derived from the empirical biome-specific NDVI relationship. Fig. 4 shows the average fPAR as derived from the MOD15 product, as well as predictions of site fPAR using the approach of Chen (1996). The results show the major effect of variable solar angle calculations on the Chen (1996) fPAR estimates and as they are computed using a constant LAI from August 2005, there are no phenological changes modelled using in this approach. By contrast the MODIS fPAR is considerably noisier due to the poor retrievals due to cloud and snow.

The inter-comparison between the EC-measured GPP values and those predicted by the 3PGS model and the MODIS GPP algorithm followed three lines of inquiry. First, we compared the 3PGS predictions of GPP, using the calibrated model with observed local meteorology, to the EC -measured GPP. This was undertaken using both the site measured fPAR (3PGS-fPAR-Site), and MODIS derived fPAR from both the MOD15 product (3PGS-fPAR-MODIS) as well as the backup algorithm as derived from coincident NDVI MODIS data (3PGS-fPAR-NDVI). In addition to a C flux comparison, the 3PGS estimates of soil water availability were compared to measured available soil water content at the site. In the second comparison with EC-measured GPP, we applied the MODIS GPP algorithm forced with local meteorology and the appropriate Biome-BGC lookup table parameters for evergreen needleleaf forest, again with site measured fPAR (MODIS-fPAR-Site), fPAR from the MOD15A product (MODIS-fPAR-MODIS) and fPAR from the backup algorithm (MODIS-fPAR-NDVI). Finally we compared EC-measured GPP with the standard MODIS GPP C4.5 product (as publicly available, derived using the DAO meteorological data and the MOD15 fPAR (MODIS17 C4.5)).

4.1. Comparison of 3PGS and EC-measured GPP

A comparison of the 3PGS predictions of GPP over the 5 years, at an 8-day time step, using local meteorology and various estimates of fPAR, with EC-measured GPP indicates a close correspondence between the two (Fig. 5(A)–(B) and Table 2). The coefficient of determination (r^2) between the observed and modeled GPP with site fPAR derived using Chen (1996) is 0.86 ($p<0.001$), with a standard error of 0.0009 kg C m^{-2} day^{-1} (Table 2). A t-test for independent samples indicates that the two sets of observations (Fig. 5A) are not significantly different ($p<0.001$) with no significant bias at either high or low GPP

Table 3
Correlations coefficients (r) between EC-measured, 3PGS or MODIS predicted GPP and various input meteorological and fPAR variables

GPP Prediction	MInT	Rain	Solar	VPD	Frost	fPAR Site	fPAR MODIS	fPAR NDVI
3PGS fPAR Site	0.77	−0.39	0.94	0.84	−0.50	−0.91	0.07	0.27
3PGS fPAR MODIS	0.75	−0.38	0.93	0.84	−0.47	−0.87	0.26	0.25
3PGS fPAR NDVI	0.77	−0.40	0.94	0.84	−0.49	−0.91	0.07	0.29
MODIS fPAR Site	0.86	−0.43	0.98	0.93	−0.49	−0.93	0.09	0.28
MODIS fPAR MODIS	0.81	−0.42	0.95	0.90	−0.46	−0.88	0.29	0.26
MODIS fPAR NDVI	0.86	−0.44	0.98	0.93	−0.49	−0.93	0.09	0.32
MOD17	0.86	−0.38	0.97	0.79	−0.48	−0.94	0.05	0.28
EC-measured	0.85	−0.40	0.91	0.81	−0.51	−0.96	0.02	0.28

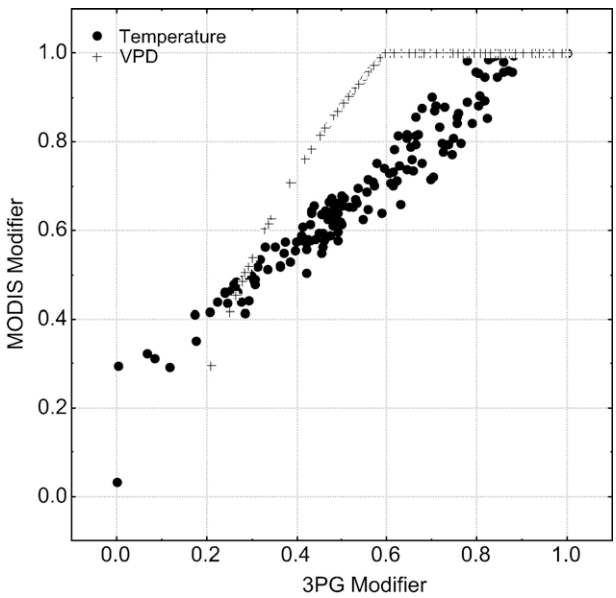

Fig. 8. Relationship between the MODIS VPD and minimum temperature modifiers with the 3PGS VPD and temperature modifiers.

levels. Computing GPP using the 3PGS model with the same calibration and meteorology, but with MOD15 fPAR (rather than site estimated fPAR), indicates a slightly poorer relationship (r^2=0.80, p<0.001), with a standard error of 0.0015 kg C m^{-2} day^{-1} (relationship not shown). The relationship remains highly significant, however a *t*-test of independent samples indicates that the EC-measured GPP and modeled estimates are significantly different (p<0.001) with the 3PGS predicted GPP being approximately 20% lower than the EC-measured GPP. The 3PGS model with fPAR derived from the MODIS NDVI backup algorithm also provided similar results (r^2=0.85, p<0.001), with a standard error of 0.0009 kg C m^{-2} day^{-1} (Table 2, Fig. 5B). For all three 3PGS simulations (fPAR site, fPAR MODIS and fPAR NDVI) the mean daily GPP was less than the mean daily EC-measured GPP (0.0044, 0.0042, 0.0045 kg C m^{-2} day^{-1} respectively compared to the EC-measured value of 0.0053 kg C m^{-2} day^{-1}). However daily variation (i.e. daily standard deviation) in the 3PGS daily GPP estimates, throughout the 5 years was always higher than that measured using EC technique (0.0036, 0.0036, 0.0037 kg C m^{-2} day^{-1} compared to 0.0035 kg C m^{-2} day^{-1}).

4.2. Soil water prediction by 3PGS

The availability of soil water and the associated vegetation response are key factors which affect GPP, since there is a close coupling between photosynthesis and the supply of water to the leaves from the soil via the roots and demand for water vapor from the leaves by the atmosphere (Leuning et al., 2005; Tuzet et al., 2003). As discussed in Heinsch et al. (2006) the MOD17 GPP algorithm uses vapor pressure deficit to account for the effects of atmospheric demand for water rather than defining and predicting soil water supply. Soils, however, provide a critical buffer between input of water as precipitation and subsequent loss by evapotranspiration. The 3PGS model predictions using local meteorology and the site based fPAR indicate that over the 5 year period available soil water is annually depleted to below 60–80% of the maximum and replenished annually (Fig. 6). Through the winter months, the soil water supply remains at full capacity. As temperature and radiation increases in April and May, the water use by the forest stand increases, the soil water supply was drawn down, to varying degrees depending on the environmental conditions. Compared to the measured available soil water content the 3PGS model predicts less water stress at the beginning of the growing season, however in all years, available soil water content decreases are observed earlier than that predicted by the 3PGS model with 3PGS predicting a quicker and later limitation of water (Fig. 6). Both datasets indicate the most significant drought occurring in 2002 and 2003 and least water stress in 2001.

4.3. Comparison of MODIS and EC-measured GPP

Compared to the 3PGS predictions, the predicted GPP using the MODIS algorithm with evergreen needleleaf biome lookup parameters, local meteorology and site determined fPAR are more highly correlated, when compared to the EC-measured GPP. The coefficient of determination (r^2) between the EC-measured and MODIS algorithm (MODIS fPAR Site) is 0.89 (p<0.001), with a standard error of 0.010 kg C m^{-2} day^{-1} (Table 2). However, a *t*-test for independent samples indicates that the two sets of observations (Fig. 5C) are significantly different (p<0.001) with a variable bias that increases with GPP. Like the 3PGS predictions, GPP estimates using the MODIS algorithm with the same calibration and local meteorology, however with MOD15 fPAR, (MODIS fPAR MODIS) results in a poorer relationship (r^2=0.80, p<0.001), with a standard error of 0.0014 kg C m^{-2} day^{-1}. The relationship (not shown) remains highly significant; however a *t*-test of independent samples again indicates the predictions and observations are significantly different (p<0.001). MODIS predictions using local climate and fPAR as estimated from the NDVI MODIS backup algorithm (MODIS fPAR NDVI), increased the strength of the relationship (r^2=0.90, p<0.001), with a standard error of 0.0011 kg C m^{-2} day^{-1} (Table 2, Fig. 5D). However, the predictions remain significantly different using an independent *t*-test from those observed (Fig. 5D) with variable bias. In all three comparisons with the MODIS algorithm, using local meteorology and variable fPAR (MODIS fPAR Site, MODIS fPAR MODIS, MODIS fPAR NDVI), the predicted mean daily GPP is always less than the EC-measured GPP (0.0039, 0.0036, 0.0040 kg C m^{-2} day^{-1} respectively, compared to the observed 0.0053 kg C m^{-2} day^{-1}). Likewise the variation (standard deviation) in daily GPP, as predicted using the MODIS algorithm, throughout the 5 years is always less than that in the EC-measured GPP (0.0030, 0.0030, 0.0030 kg C m^{-2} day^{-1} respectively versus 0.0035 kg C m^{-2} day^{-1} observed).

Finally we consider the MODIS GPP C4.5 product (available online and calculated using the DAO meteorological data with either the quality assured MODIS MOD15A2 fPAR (17% of cases) or fPAR from the backup NDVI algorithm). Results

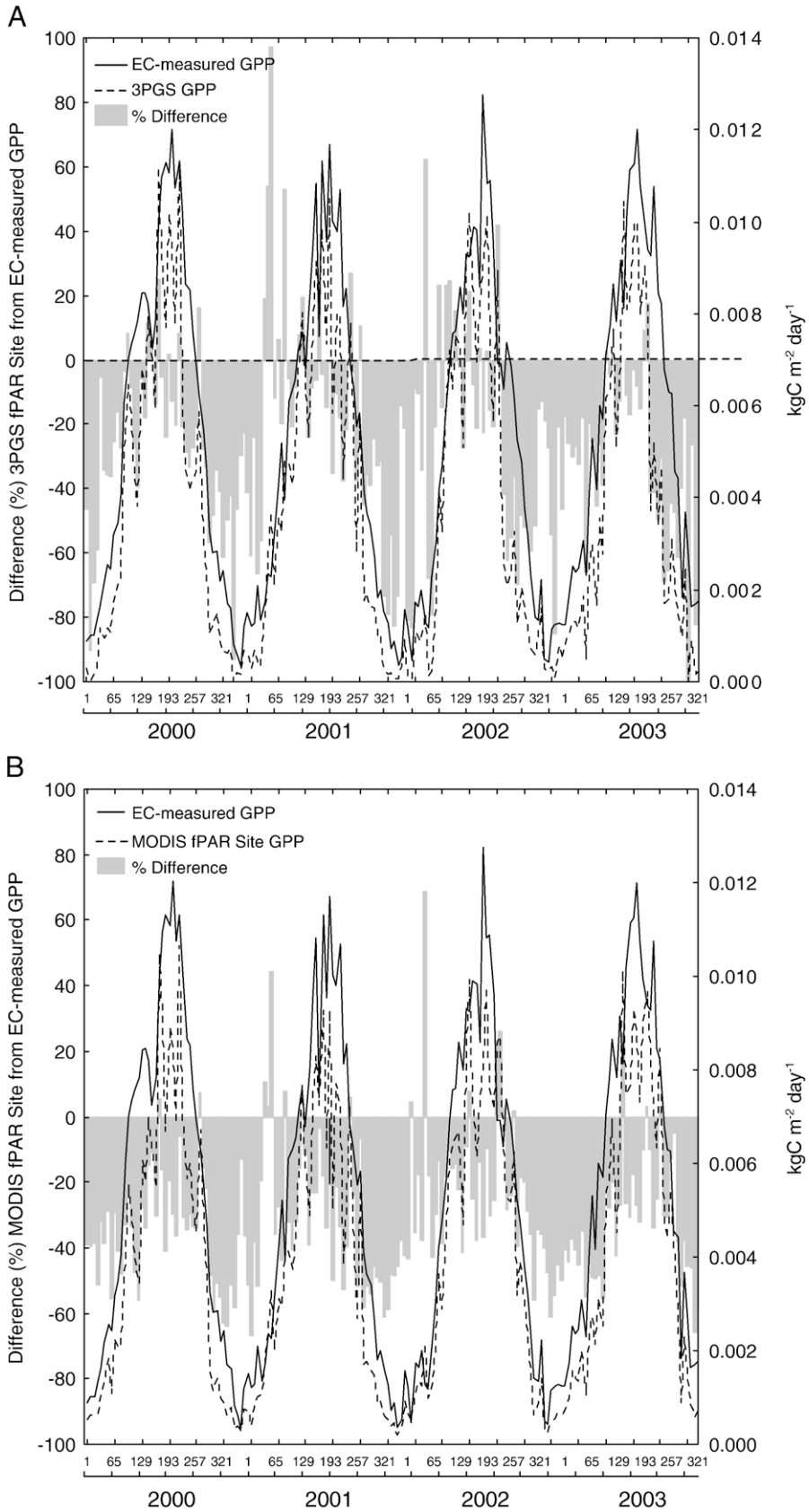

Fig. 9. (A)–(C): Temporal trace of the 8-day observed EC-measured GPP and the percent difference between the observed and three model GPP predictions: (A) 3PGS with site estimated fPAR and local meteorology, (B) MODIS with local meteorology and site measured fPAR and (C) GPP as predicted by the MOD17.

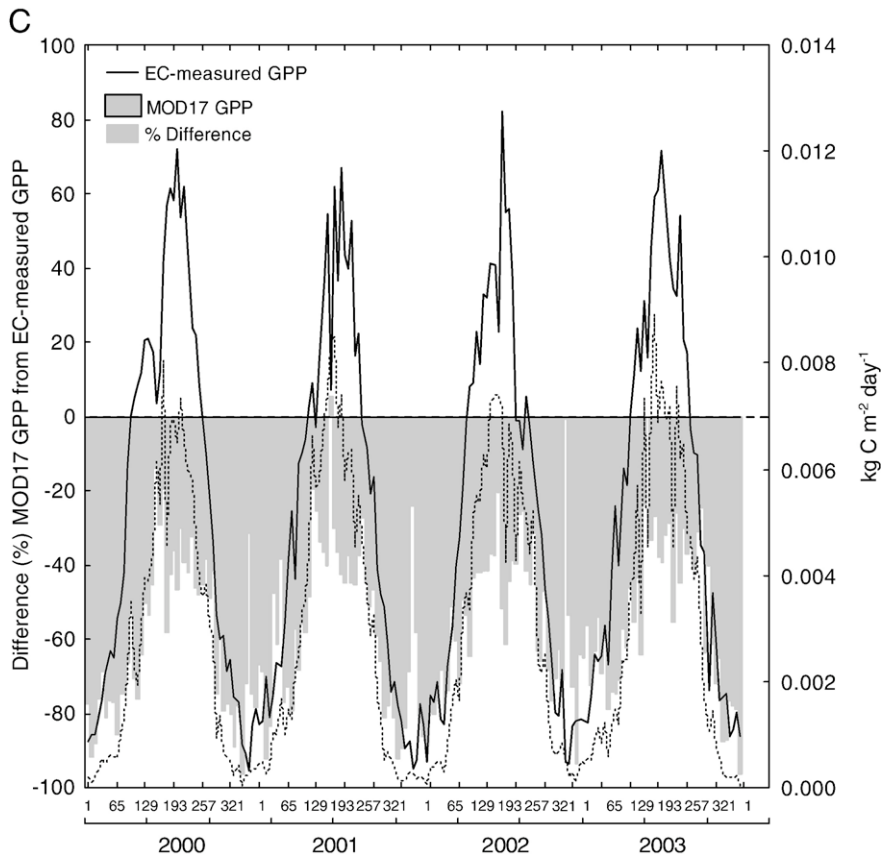

Fig. 9 (*continued*).

indicate the relationship between the EC-measured and modeled GPP remains high $r^2=0.88$ ($p<0.001$), with a standard error of 0.0010 kg C m^{-2} day^{-1} (Fig. 7). A *t*-test for independent samples indicates that the two sets of observations are significantly different ($p<0.001$). The MODIS C4.5 GPP estimates averaged over the 4 years are approximately 30% less that the EC measurements (0.0029 kg C m^{-2} day^{-1} compared to the EC-measured 0.0052 kg C m^{-2} day^{-1}) (Table 2).

4.4. Correlation of 3PGS, MODIS, and EC-measured GPP with meteorological variables

From correlation analysis of the overall effect of each of the input meteorological variables on the variation of 8-day observed GPP, it is apparent that 86% ($r=0.93$–0.94) of the variation in the 3PGS predicted GPP can be explained by the variation in total incoming solar radiation (Solar—Table 3). By contrast, 84% ($r=0.91$) of the variation in EC-measured GPP is explained by the variation in total incoming solar radiation. Likewise the site estimated fPAR, compared to the fPAR estimated using the MODIS backup algorithm (derived from MODIS NDVI) and the MOD15 fPAR product, explained a larger amount of the EC-measured, and 3PGS and MODIS modeled GPP. Of the other climatic variables, there is a moderate positive relationship with VPD and minimum temperature. In the case of minimum temperature, this correlation is highest with the EC-measured GPP, followed by the MODIS GPP, and is weakest with 3PGS GPP predictions. In all cases, 8-day accumulated rainfall and frost are negatively related to the EC-measured or 3PGS and MODIS modeled GPP. Interestingly there is a common negative correlation between all estimates of GPP and annual rainfall. While this relationship is only moderate in strength one possible reason is that water is only a key limiting factor to growth at selected times of year. For the remainder of the year however increases in radiation and temperature drive growth, and when increases in these variables occur, it is often associated with reductions rather than increases in precipitation.

The consistent underestimation in GPP based on the MODIS algorithm compared to both the 3PGS predictions and the EC-measured GPP, given the same input meteorology and fPAR observations, indicates the MODIS GPP biome parameters for evergreen needleleaf forests may be biased in this very high productivity Douglas-fir forest. The relationships between the MODIS VPD and minimum temperature modifiers with the 3PGS VPD and temperature modifiers are shown in Fig. 8. In 3PGS the temperature modifier is based on a polynomial function with minimum, maximum and optimum temperature constraints. In the case of the MODIS algorithm the temperature function is a simple function of daily minimum temperature. The results indicate that throughout the range of modifier from no restriction to growth (1) to no growth (0), the 3PGS algorithm

covers the full range from 0 to 1 whereas the MODIS temperature function does not cover the full range but is limited to between 0.3 and 1. Likewise, the VPD modifier in the case of the 3PGS again goes between 1 and 0, whereas in the case of the MODIS algorithm, there is a smaller range with a much stronger relationship resulting in a shorter range of VPD modification for the MODIS predictions than for 3PGS.

4.5. Comparison of seasonal variation in 3PGS, MODIS, and observed EC-measured GPP

One of the key strengths of the 3PGS and MODIS GPP predictions is their capacity to capture seasonal dynamics in photosynthetic production. As a result seasonal traces of 3PGS and MODIS GPP at the site were compared with EC-measured GPP at the tower. The results show the EC-measured GPP and the percent difference between the three sets of model predictions (3PGS fPAR Site, MODIS fPAR Site, and MOD17 GPP (Fig. 9(A)–(C)). The results indicate that, for the 3PGS estimates, the times of the largest differences in prediction are in the winter months where the difference can be as large as 80% with the EC-measured GPP always being larger than modelled. During the growing season the differences are reduced and are often less than 20%. The dynamics of the growing season are best matched in 2000 and 2001 where both the onset and end of the growing season is captured. This is an important result as spring is the time of growing season onset, and there is a relatively rapid transition in ecosystem processes. In 2003 both 3PGS and the MODIS algorithm with local parameters predicted the commencement of the growing season later than observed using the EC data. Overall however, the MODIS estimated GPP using local meteorology and site fPAR is always underestimating the EC-measured GPP, with relative differences also larger (40%) in the winter months than in the summer (<20%). In case of the MOD17 GPP, the algorithm predicts a much shorter growing season than the one predicted by the EC-measured values and starts the onset of the growing season late and finishes it early. The year with the best correspondence is 2001. Overall, all three sets of predictions have some periods of large differences in spring. With an 8-day compositing period used by the MODIS algorithm both in the GPP predictions, as well as fPAR/NDVI relations, it is not surprising that some of the greatest differences between EC and MODIS estimates of GPP occur during this period. In a detailed examination of sites across North America, Heinsch et al. (2006) found that MODIS C4.5 data corresponded less well in spring.

4.6. Observed nighttime respiration and MODIS land surface temperature

Lastly we show a relationship between nighttime ecosystem respiration measured in the first 2 years at the tower site with the minimum 8-day MODIS land surface temperature. Functional relationships between soil temperature, moisture, and respiration have been described for soils in mature, upland boreal forests (Moosavi & Crill, 1997) as well as Douglas-fir forests (Morgenstern et al., 2004). As a result a general positive relationship would be expected between soil temperature and ecosystem respiration. The ability to derived 8-day average minimum temperature for the globe provides some hope in the derivation of, at least, a component of the ecosystem respiration for use in globe productivity modeling. The relationship between nighttime respiration and minimum 8-day MODIS land surface temperature is shown in Fig. 10 and shows a general exponential trend. The relationship is significant ($r^2=0.57$) with a similar functional form to that found by Rahman et al. (2005), however the latter predicts lower nighttime respiration at warmer temperatures which may in part be due to the wetter climate and subsequently wetter soils compared to other sites.

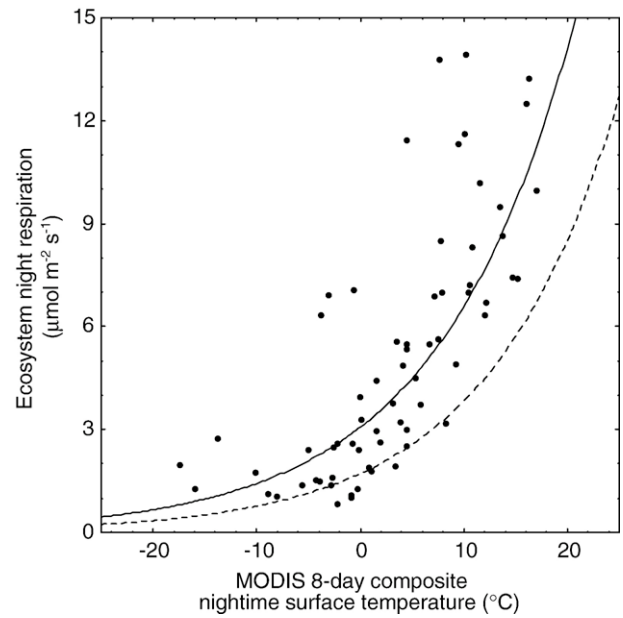

Fig. 10. Relationship between nighttime ecosystem respiration measured by EC (μmol m^{-2} s^{-1}) and minimum 8-day MODIS land surface temperature. Relationship is a general exponential trend, with a regression fit shown as a solid line. The dashed line shows the relationship developed by Rahman et al. (2005).

5. Discussion

In this paper we examined the degree of correspondence between the EC-measured GPP and that predicted by the MODIS operational algorithm (C4.5), which uses broad scale DAO meteorology, and general biome specific calibration. In addition, we compared predictions by the MODIS algorithm with local meteorological and fPAR observations, as well as predictions made by a simple physiological model (3PGS). Differences in both the model predictions and the EC-measured GPP are expected. The EC measurements themselves are not free from error. EC-measured GPP is estimated as the sum of daytime NEP and ecosystem respiration (i.e., R_d); where the latter is computed from the nighttime relationship between EC-measured NEE and temperature. It has been reported that since the EC-method derives daytime respiration using nighttime flux–temperature relationships ignoring the reduction in leaf respiration in light relative to darkness (i.e., photoinhibition), the EC-method can thus consistently overestimate GPP (e.g. Janssen et al., 2001; Reichstein et al.,

2005; Wohlfahrt et al., 2005). These biases are also likely to be true at this site with the EC-measured GPP possibly overestimated up to 20%. Similarly the heterogeneity of the surrounding terrain is also an issue with EC estimation of GPP. If this consistent overestimation of GPP is in fact accurate, then the observed differences between the MODIS and 3PGS modeled GPP and the EC-measured GPP will be greatly reduced and in most cases result in a near 1:1 relationship.

Two key sets of variables have significant effects on the prediction of GPP in this study: the input observations of fPAR and local meteorology. It is apparent both in this and previous work, that the accuracy of the MODIS GPP data is highly dependent on the MODIS fPAR product and that retrieval of leaf area and fPAR under conditions with low solar angles, persistent cloud cover, and snow is exceptionally difficult. The climate in the Pacific Northwest is that of a temperate rainforest and even in the summer months, the area can experience significant rainfall. As a result, extraction of a high quality fPAR data for each of the 8-day time intervals can be problematic. In fact the success rate of a quality assured fPAR retrieval is less than 20% for our site over the 5-year period. Even with the improved filtering of the fPAR product prior to use with the MOD17 GPP predictions it is still possible that the MODIS algorithm requires fPAR data estimated from the NDVI backup algorithm. In this case the overall results are not significantly effected with similar relationship between the MODIS and EC-measured GPP, likely due to the consistently high LAI at the Douglas-fir site and subsequently very large fPAR values (>90%). As indicated by Chen (1996), fPAR itself does vary seasonally however by less than 5%, as shown in Fig. 4. When extracting the MODIS fPAR data, it is apparent that much of the variation observed is due to viewing conditions, which would be expected to reduce the relationship between EC-measured and MODIS GPP. By using observed fPAR at the high and constant levels, the major driver of the GPP at the site, and in the predictions, is based on absorbed photosynthetically active radiation (APAR) rather than reductions due to fPAR.

The second largest error associated with MOD17 GPP product derives from the meteorology (Zhao et al., 2006). The MOD17 algorithm is strongly dependent on VPD to reduce the maximum radiation use efficiency, and therefore, an underestimation VPD would result in a large overestimation of GPP. It is known that the DAO meteorology underestimates local VPD in many dry sites during the summer, and thus does not sufficiently constrain photosynthesis in the MOD17 algorithm during dry periods in North America (Heinsch et al., 2006; Zhao et al., 2006). In this example, however all sets of predictions underestimate the EC-measured GPP, as was the case at the Duke forest site (Heinsch et al., 2006). An underestimation of the ε used by the MODIS algorithm, a highly heterogeneous landscape due to the plantation forestry activities, as well as an incorrect land cover classification (mixed forest instead of evergreen needleleaf forest) were proposed as the main reasons for the under-prediction. In the present study, the land cover classification is correct, however like Heinsch et al. (2006) values of α in the 3PGS model (equivalent to ε in the MODIS algorithm) were higher than other studies (Waring & McDowell, 2002) however still well within variation measured at other evergreen needleleaf sites (0.0005–0.0028 kg C MJ^{-1}) (Turner et al., 2003).

Despite these differences however, the results presented here indicate that both the 3PGS and MODIS models, driven using site and satellite based observations, produce highly accurate estimates when compared to the EC-measured GPP. Given the extensive land area occupied by Douglas-fir in western North America these results confirm the usefulness of these datasets in the ongoing monitoring of the terrestrial ecosystem and provision of continuous measurements of vegetation production.

Acknowledgements

We are grateful to Andrew Eisenberg for significant programming assistance. Campbell River site flux tower measurements are partly funded by the FLUXNET Canada program through the Natural Science and Engineering Research Council of Canada, BIOCAP Canada and the Canadian Foundation for Innovation. In addition, funding is provided by the Canadian Forest Service (CFS). We are grateful to Jing Chen (University of Toronto) for access to his LAI observations at the site. Components of this research were also funded by a NSERC Discovery grant to Coops. Preparation of the combined forest inventory was done partially through Action Plan 2000 and FLUXNET–CCAF funding to T. Trofymow. Finally, we are grateful to the two anonymous reviewers who provided editorial suggestions.

References

Baldocchi, D. (1997). Measuring and modeling carbon dioxide and water vapour exchange over a temperate broad-leaved forest during the 1995 summer drought. *Plant Cell and Environment*, *20*, 1108−1122.

Baldocchi, D., Falge, E., Gu, L., Olson, R., Hollinger, D., Running, S. W., et al. (2001). FLUXNET: A new tool to study the temporal and spatial variability of ecosystem-scale carbon dioxide, water vapor, and energy flux densities. *Bulletin of the American Meteorological Society*, *82*, 2415−2434.

Barford, C. C., Wofsy, S. C., Goulden, M. L., Munger, J. W., Hammond Pyle, E., Urbanski, S. P., et al. (2001). Factors controlling long-and short-term sequestration of atmospheric CO_2 in a mid-latitude forest. *Science*, *294*, 1688−1691.

Barr, A. G., Black, T. A., Hogg, E. H., Kljun, N., Morgenstern, K., & Nesic, Z. (2004). Inter-annual variability in the leaf area index of a boreal aspen–hazelnut forest in relation to net ecosystem production. *Agricultural and Forest Meteorology*, *126*, 237−255.

Black, T. A. (1979). Evaporation from Douglas-fir stands exposed to soil water deficits. *Water Resources Research*, *15*, 164−170.

Campbell, G. S, & Norman, J. M. (1998). *An introduction to environmental physics* (pp. 286). New York: Springer.

Chen, J. M. (1996). Canopy architecture and remote sensing of the fraction of photosynthetically active ration absorbed by boreal conifer forests. *IEEE Transactions on Geoscience and Remote Sensing*, *34*, 1353−1368.

Chen, J.M., Govind, A., Sonnentag, O., Zhang, Y., Barr, A., & Amiro, B. (in press). Leaf area index measurements at FLXUNET Canada forest sites. *Agricultural and Forest Meteorology.*

Coops, N. C., & Waring, R. H. (2001a). The use of multi-scale remote sensing imagery to derive regional estimates of forest growth capacity using 3-PGS. *Remote Sensing of Environment*, *75*, 324−334.

Coops, N. C., & Waring, R. H. (2001b). Estimating maximum potential site productivity and site water stress of the eastern Siskiyous using 3-PGS. *Canadian Journal of Forest Research*, *31*, 143−154.

Coops, N. C., Waring, R. H., & Landsberg, J. J. (1998). Assessing forest productivity in Australia and New Zealand using a physiologically-based

model driven with averaged monthly weather data and satellite derived estimates of canopy photosynthetic capacity. *Forest Ecology and Management*, *104*, 113−127.

DAO (2002). *Data Assimilation Office (DAO) Algorithm Theoretical Basis Document (ATBD)*. Greenbelt, MD: Data Assimilation Office, Goddard Space Flight Center.

Foti, S., Cosentino, L., Patan, C., Copani, V., & Sanzone, E. (2003). Plant indicators of available soil water in the perennial herbaceous crop Miscanthus · giganteus Greef et Deu. *Agronomie*, *23*, 29−36.

Friend, A. D. (1995). PGEN: An integrated model of leaf photosynthesis, transpiration, and conductance. *Ecological Modelling*, *77*, 233−255.

Garcia-Quijano, J., & Barros, A. P. (2005). Incorporating vegetation dynamics into a hydrological model: Photosynthesis, dynamic respiration and stomatal sensitivity. *Ecological Modelling*, *185*, 29−49.

Gebremichael, M., & Barross, A. P. (2006). Evaluation of MODIS gross primary productivity (GPP) in tropical monsoon regions. *Remote Sensing of Environment*, *100*, 150−166.

Goodwin, G. (1937). Regeneration Study on the logged-off lands of the Comox Logging and Railway Company Oyster River, Forest Survey No. R 72, Survey file No. 0124780 BC Forest Service. 39p and Map.

Goulden, M. L., Munger, J. W., Fan, S., Daube, B. C., & Wofsy, S. C. (1996). Measurements of carbon sequestration by long-term eddy covariance: Methods and a critical evaluation of accuracy. *Global Change Biology*, *2*, 169−182.

Green, R. N., & Klinka, K. (1994). *A field guide to site identification and interpretation for the Vancouver forest region: Land management handbook # 28.* Victoria: Province of British Columbia.

Griffis, T. J., Black, T. A., Morgenstern, K., Barr, A. G., Nesic, Z., Drewitt, G. B., et al. (2003). Ecophysiological controls on the carbon balances of three southern boreal forests. *Agriculture and Forest Meteorology*, *125*, 207−223.

Hansen, M. C., DeFries, R. S., Townshend, J. R. G., & Sohlberg, R. (2000). Global land cover classification at 1 km spatial resolution using a classification tree approach. *International Journal of Remote Sensing*, *21*, 1331−1364.

Heinsch, F. A., Zhao, M., Running, S. W., Kimball, J. S., Nemani, R. R., Davis, K. J., et al. (2006). Evaluation of remote sensing based terrestrial productivity from MODIS using regional tower eddy flux network observations. *IEEE Transactions on Geoscience and Remote Sensing*, *44*, 1908−1925.

Hook, W. R., & Livingston, N. J. (1996). Errors in converting time domain reflectometry measurements of propagation velocity to estimates of soil water content. *Soil Science Society of America Journal*, *60*, 35−41.

Humphreys, E. R., Black, T. A., Morgenstern, K., Cai, T., Drewitt, G. B., & Nesic, Z. (in press). Carbon dioxide fluxes in three coastal Douglas-fir stands at different stages of development after harvesting. *Agricultural and Forest Meteorology.*

IPCC (2001). Climate change 2001: The scientific basis. In J. T. Houghton, Y. Ding, D. J. Griggs, M. Noguer, P. J. van der Linden, X. Dai, K. Maskell, & C. A. Johnson (Eds.), *Contribution of working group 1 to the third assessment report of the intergovernmental panel on climate change* (pp. 882). Cambridge: Cambridge University Press.

Janssen, I. A., Lankreijer, H., Matteucci, G., Kowalski, A. S., Buchmann, N., Epron, D., et al. (2001). Productivity overshadows temperature in determining soil and ecosystem respiration across European forests. *Global Change Biology*, *7*, 269−278.

Jungen, J. R. (1985). *Soils of southern Vancouver Island. British Columbia surveys and resource mapping branch.* Victoria, B.C.: Ministry of Environment.

Knyazikhin, Y., Glassy, J., Privette, J. L., Tian, Y., Lotsch, A., Zhang, Y., et al. (1999). MODIS leaf area index (LAI) and fraction of photosynthetically active radiation absorbed by vegetation (FPAR) product (MOD15) algorithm theoretical basis document, http://www.ntsg.umt.edu/modis/ATBD/ATBD_MOD15_v21.pdf. Last accessed April 2006.

Landsberg, J. J., & Gower, S. T. (1997). *Applications of physiological ecology to forest management* (pp. 354). San Diego, California: Academic Press.

Landsberg, J. J., & Waring, R. H. (1997). A generalized model of forest productivity using simplified concepts of radiation-use efficiency, carbon balance and partitioning. *Forest Ecology and Management*, *95*, 209−228.

Leblanc, S. G., & Chen, J. M. (2001). A practical scheme for correcting multiple scattering effects on optical LAI measurements. *Agricultural and Forest Meteorology*, *110*, 125−139.

Leuning, R., Cleugh, H., Zegelin, S., & Hughes, D. (2005). Carbon and water fluxes over a temperate Eucalyptus forest and a tropical wet/dry savanna in Australia: Measurements and comparison with MODIS remote sensing estimates. *Agricultural and Forest Meteorology*, *129*, 151−173.

Lewis, J. D., Olysyk, D., & Tingey, D. T. (1999). Seasonal patterns of photosynthetic light response in Douglas-fir seedlings subjected to elevated atmospheric CO_2 and temperature. *Tree Physiology*, *19*, 243−252.

McMurtrie, R. E., Rook, D. A., & Kelliher, F. M. (1990). Modelling the yield of *Pinus radiata* on a site limited by water and nitrogen. *Forest Ecology and Management*, *30*, 381−413.

Monteith, J. L. (1966). The photosynthesis and transpiration of crops. *Experimental Agriculture*, *2*, 1−14.

Monteith, J. L. (1972). Solar radiation and productivity in tropical ecosystems. *Journal of Applied Ecology*, *9*, 747−766.

Moosavi, S. C., & Crill, P. M. (1997). Controls of CH4 and CO2 emissions along two moisture gradients in the Canadian boreal zone. *Journal of Geophysical Research*, *102*(D4), 29261−29277.

Morgenstern, K., Black, T. A., Humphreys, E. R., Griffis, T. J., Drewitt, G. B., Cai, T., et al. (2004). Sensitivity and uncertainty of the carbon balance of a Pacific Northwest Douglas-fir forest during an El Niño/La Niña cycle. *Agricultural and Forest Meteorology*, *123*, 201−219.

Myneni, R. B., Hoffman, S., Knyazikhin, Y., Privette, J. L., Glassy, J., Tian, Y., et al. (2002). Global products of vegetation leaf area and fraction absorbed PAR from year one of MODIS data. *Remote Sensing of Environment*, *83*, 214−231.

Nemani, R. R., Keeling, C. D., Hashimoto, H., Jolly, W. M., Piper, S. C., Tucker, C. J., et al. (2003). Climate-driven increases in global terrestrial net primary production from 1982 to 1999. *Science*, *300*, 1560−1563.

Nemani, R. R., White, W., Thornton, P., Nishida, K., Reddy, S., Jenkins, S., et al. (2002). Recent trends in hydrologic balance have enhanced the terrestrial carbon sink in the United States. *Geophysical Research Letters*, *29*(10), 106-1−106-4.

Pojar, J., Klinka, K., & Demarchi, D. A. (1991). Chapter 6: Coastal western hemlock zone. In D. Meidinger & J. Pojar (Eds.), *Ecosystems of British Columbia. BC Special Report Series*, *Vol. 6*. (pp. 95−111) Victoria: BC Ministry of Forests.

Rahman, A. F., Sims, D. A., Cordova, V. D., & El-Masri, B. Z. (2005). Potential of MODIS EVI and surface temperature for directly estimating per-pixel ecosystem carbon fluxes. *Geophysical Research Letters*, *32* (L19404) (4 pages).

Reichstein, M., Falge, E., Baldocchi, D., Papale, D., Aubinet, M., Berbigier, P., et al. (2005). On the separation of net ecosystem exchange into assimilation and ecosystem respiration: Review and improved algorithm. *Global Change Biology*, *11*, 1424−1439.

Reichstein, M., Tenhunen, J. D., Roupsard, O., Ourcival, J. -M., Rambal, S., Miglietta, F., et al. (2002). Severe drought effects on ecosystem CO2 and H2O fluxes at three Mediterranean evergreen sites: Revision of current hypotheses? *Global Change Biology*, *8*, 999−1017.

Running, S. W., & Coughlan, J. C. (1988). A general model of forest ecosystem processes for regional applications: I. Hydrologic balance, canopy gas exchange and primary production processes. *Ecological Modelling*, *42*, 125−154.

Running, S. W., & Gower, S. T. (1991). FOREST-BGC, a general model of forest ecosystem processes for regional applications II: Dynamic carbon allocation and nitrogen budgets. *Tree Physiology*, *9*, 147−160.

Running, S. W., Nemani, R. R., Heinsch, F. A., Zhao, M., Reeves, M., & Jolly, M. (2004). A continuous satellite-derived measure of global terrestrial primary productivity: Future science and applications. *Bioscience*, *56*(6), 547−560.

Schimel, D. (1995). Terrestrial biogeochemical cycles: Global estimates with remote sensing. *Remote Sensing of Environment*, *51*, 49−56.

Tian, Y., Wang, Y., Zhang, Y., Knyazikhin, Bogaert, J., & Myneni, R. B. (2002). Radiative transfer based scaling of LAI/FPAR retrievals from reflectance data of different resolutions. *Remote Sensing of Environment*, *84*, 143−159.

Turner, D. P., Ritts, W. D., Cohen, W. B., Gower, S. T., Zhao, M., Running, S. W., et al. (2003). Scaling gross primary production (GPP) over boreal and deciduous forest landscapes in support of MODIS GPP product validation. *Remote Sensing of Environment*, *88*, 256−270.

Turner, D. P., Ritts, W. D., Cohen, W. B., Maeirsperger, T. K., Gower, S. T., Kirschbaum, A. A., et al. (2005). Site-level evaluation of satellite-based global terrestrial GPP and NPP monitoring. *Global Change Biology*, *11*, 666−684.

Tuzet, A., Perrier, A., & Leuning, R. (2003). Stomatal control of photosynthesis and transpiration: Results from a soil–plant–atmosphere continuum model. *Plant Cell and Environment*, *26*, 1097−1116.

Waring, R. H., & McDowell, N. G. (2002). Use of a physiological process model with forestry yield tables to set limits on annual carbon balances. *Tree Physiology*, *22*, 179−188.

White, M. A., Thornton, P. E., Running, S. W., & Nemani, R. (2000). Parameterization and sensitivity analysis of the BIOME-BGC terrestrial ecosystem model: Net primary production controls. *Earth Interactions*, *4*, 1−55.

Wofsy, S. C., Goulden, M. L., Munger, J. W., Fan, S. M., Bakwin, P. S., Daube, B. C., et al. (1993). Net exchange of CO2 in a midlatitude forest. *Science*, *260*, 1314−1317.

Wohlfahrt, G., Bahn, M., Haslwanter, A., Newesely, C., & Cernusca, A. (2005). Estimation of daytime ecosystem respiration to determine gross primary production of a mountain meadow. *Agricultural and Forest Meteorology*, *130*, 13−25.

Yang, W., Huang, D., Tan, B., Stroeve, J., Shabanov, N. V., Knyazikhin, Y., et al. (2006). Analysis of leaf area index and fraction of PAR absorbed by vegetation products from the terra MODIS sensor: 2000–2005. *IEEE Transactions on Geoscience and Remote Sensing*, *44*, 1829−1842.

Zhao, M., Heinsch, F. A., Nemani, R. R., & Running, S. W. (2005). Improvements of the MODIS terrestrial gross and net primary production global dataset. *Remote Sensing of Environment*, *95*, 164−176.

Zhao, M., Running, S. W., & Nemani, R. R. (2006). Sensitivity of moderate resolution imaging spectroradiometer (MODIS) terrestrial primary production to the accuracy of meteorological reanalyses. *Journal of Geophysical Research*, *111*(G01002). doi:10.1029/2004JG000004.6